HHS Public Access

Author manuscript

J Bone Miner Res. Author manuscript; available in PMC 2018 April 01.

Published in final edited form as:

J Bone Miner Res. 2017 April ; 32(4): 821–833. doi:10.1002/jbmr.3045.

FLUOXETINE INHIBITS OSTEOBLAST DIFFERENTIATION & MINERALIZATION IN FRACTURE HEALING:

The Selective Serotonin Reuptake Inhibitor Fluoxetine Directly Inhibits Osteoblast Differentiation and Mineralization During Fracture Healing in Mice

Vivian Bradaschia-Correa[1], **Anne M Josephson**[1], **Devan Mehta**[1], **Matthew Mizrahi**[1], **Shane S Neibart**[1], **Chao Liu**[1,2], **Oran Kennedy**[1,2], **Alesha B Castillo**[1,2], **Kenneth A Egol**[1], and **Philipp Leucht**[1,3]

[1]Department of Orthopaedic Surgery, Langone Medical Center–Hospital for Joint Diseases, New York University, New York, NY, USA

[2]Department of Mechanical and Aerospace Engineering, Tandon School of Engineering, New York University, New York, NY, USA

[3]Department of Cell Biology, School of Medicine, New York University, New York, NY, USA

Abstract

Chronic use of selective serotonin reuptake inhibitors (SSRIs) for the treatment of depression has been linked to osteoporosis. In this study, we investigated the effect of chronic SSRI use on fracture healing in two murine models of bone regeneration. First, we performed a comprehensive analysis of endochondral bone healing in a femur fracture model. C57/BL6 mice treated with fluoxetine, the most commonly prescribed SSRI, developed a normal cartilaginous soft-callus at 14 days after fracture and demonstrated a significantly smaller and biomechanically weaker bony hard-callus at 28 days. In order to further dissect the mechanism that resulted in a smaller bony regenerate, we used an intramembranous model of bone healing and revealed that fluoxetine treatment resulted in a significantly smaller bony callus at 7 and 14 days postinjury. In order to test whether the smaller bony regenerate following fluoxetine treatment was caused by an inhibition of osteogenic differentiation and/or mineralization, we employed in vitro experiments, which established that fluoxetine treatment decreases osteogenic differentiation and mineralization and that this effect is serotonin-independent. Finally, in a translational approach, we tested whether cessation of the medication would result in restoration of the regenerative potential. However, histologic and μCT analysis revealed non-union formation in these animals with fibrous tissue interposition within the callus. In conclusion, fluoxetine exerts a direct, inhibitory effect on osteoblast differentiation and mineralization, shown in two disparate murine models of bone repair. Discontinuation of the drug did not result in restoration of the healing potential, but rather

Address correspondence to: Philipp Leucht, MD, Departments of Orthopaedic Surgery and Cell Biology, New York University School of Medicine, 550 First Avenue, MSB-617, New York, NY 10016, USA. philipp.leucht@nyumc.org.

Additional Supporting Information may be found in the online version of this article.

Authors' roles: Study design: KAE and PL. Study conduct: VBC, AMJ, DM, MM, SSN, and CL. Data collection: VBC, AMJ, DM, MM, SSN, and CL. Data analysis: VBC, ABC, and PL. Data interpretation: VBC and PL. Drafting manuscript: PL. Approving final version of manuscript: VBC, AJM, DM, MM, SSN, CL, ODK, ABC, and KAE. PL takes responsibility for the integrity of the data analysis.

led to complete arrest of the repair process. Besides the well-established effect of SSRIs on bone homeostasis, our study provides strong evidence that fluoxetine use negatively impacts fracture healing.

Keywords

OSTEOPOROSIS; DEPRESSION; OSTEOBLAST; OSTEOPROGENITOR CELL; BONE

Introduction

A 2010 report from the Center for Disease Control and Prevention's (CDC) National Health and Nutrition Examination Survey (NHANES) tracking antidepressant use among Americans from 2005 to 2008 found that more than 1 in 10 Americans ages 12 and older report taking an antidepressant medication.[1] About 254 million prescriptions are written for antidepressants in 1 year, resulting in nearly $10 billion in costs.[2]

Selective serotonin reuptake inhibitors (SSRIs) antagonize the serotonin transporter (5-HTT), and are currently the most commonly prescribed antidepressant on the US market. Recent findings have identified a functional role of the serotonin signaling pathway in bone cells,[3] which is likely responsible for the observed increase in the incidence of osteoporosis in patients on long-term SSRI treatment.[4] The exact mechanism underlying this SSRI-dependent bone loss is unknown, but some evidence exists indicating a negative effect on bone matrix deposition.[1,5] A genetic knockout of 5-HTT in adolescent mice as well as oral treatment with an SSRI resulted in impaired bone mineral accrual. Both approaches resulted in a reduction in overall bone formation during bone homeostasis and growth without affecting bone resorption.[6]

The majority of the body's serotonin is taken up by the platelets after it is synthesized in the gastrointestinal tract.[7] The remainder is circulating unbound in the serum, from where it diffuses into tissues, such as the skeleton. In patients taking SSRIs, free serotonin is inhibited from reuptake into platelets and other cells, which results in an overall increase in serotonin in tissues, including bone.[4] This increased tissue level serotonin concentration is thought to be responsible for the bone phenotype. Recent research has shown that as a result of the catabolic effect on bone, patients within the first 8 months of SSRI treatment are at an increased risk of fracture.[3]

Osteoporosis results in a biomechanically weakened skeleton, which is prone to fracture. Treating osteoporotic fractures can be challenging, because the decrease in bone density makes implant fixation more difficult. Therefore, any delay in bone healing, resulting from medications such as SSRIs, will increase the chance of implant failure due to excessive construct strain, and may therefore result in suboptimal outcome.

Chronic SSRI use has been linked to the development of osteoporosis by inhibiting bone matrix deposition.[1,4,8] Osteoblastic differentiation and osteoid deposition during bone homeostasis represents a very slow and continuous process. Thus, if the chronic use of SSRIs leads to a detectable change in bone matrix deposition during homeostasis, then it is

very likely that this negative effect is exacerbated in the faster, more dynamic process of fracture repair. The majority of fractures encountered by orthopedic patients heal through endochondral ossification. Therefore, we first utilized a murine model of endochondral ossification to study the effect of chronic fluoxetine use[9] on this mode of repair.

We hypothesized that SSRIs exert a negative effect on osteoblast proliferation and differentiation during the process of fracture repair. We approached this hypothesis by first dissecting the effect of fluoxetine on the complex program of bone regeneration in two disparate models of fracture repair, followed by an in-depth analysis of SSRI effects on osteoprogenitor cells (OPCs) in vitro.

Materials and Methods

Fluoxetine treatment

All procedures were approved by the New York University Committee on Animal Research. Studies were conducted on 12 week-old C57BL/6 male mice (*Mus musculus*) purchased from Jackson Laboratory (Bar Harbor, ME, USA). Mice were maintained on a 12-hour light/dark cycle with food and water provided *ad libitum*.

Fluoxetine (Teva Pharmaceuticals, Sellersville, PA, USA) was delivered in the drinking water. Mice were randomly selected to either receive treatment or control fluid. A 240 mg/L fluoxetine solution was prepared so that the mice received 10 mg/kg/day.[9] To simulate chronic fluoxetine use, mice received oral treatment for 3 weeks before the surgical procedures[9] and their treatment was continued until euthanasia. Body weight of the mice was assessed before, during, and after treatment, and was found to be unaffected by the treatment. An additional group had the fluoxetine treatment discontinued on the day of fracture surgery and received regular drinking water during the following 4 weeks (termed “fluoxetine discontinued” in text and figure legends).

Surgical procedures

In order to model bone repair through endochondral ossification, an established femur fracture model with intramedullary stabilization was employed.[10] Briefly, after anesthesia was induced with isoflurane inhalation (1% to 5%), an incision was made along the anterolateral femur. On the medial side of the patella tendon, a 27G syringe needle was inserted through the distal femoral metaphysis into the medullary canal. The needle was partially removed and the mid-diaphysis of the femur was transected with small surgical scissors. The needle was reinserted into the femur to stabilize the fracture. The free edge of the muscle flap was placed over the injury site with a single stitch, and skin was closed. Mice were euthanized by CO_2 asphyxiation, followed by cervical dislocation on postoperative day (POD) 14 and 28.

Intramembranous ossification was studied using a monocortical tibial defect model, as described.[11,12]

μCT analyses

Implants were removed from the femurs prior to scanning. Specimens were scanned at 10-μm isotropic resolution using a Skyscan 1172 (Bruker, Billerica, MA, USA). The following parameters were analyzed: total bone volume (BV), total tissue volume (TV), and respective mineralized volume fraction (BV/TV) (%), trabecular number (Tb.N), trabecular thickness (Tb.Th), and trabecular separation (Tb.Sp).

Structural and compositional callus strength assessment

The maximum and minimum bending moment of inertia (I_{max} and I_{min}, respectively), as well as the polar moment of inertia (J), where $J = I_{max} + I_{min}$, were measured for the femur diaphysis, using CTan software (Bruker μCT). The volume of interest (VOI) consisted of the entire diaphysis of the femur in the longitudinal direction, and included the entire callus in the transverse direction. Thresholding was performed on the VOI to include all of the volume inside the perimeter of the fracture callus as established.[13] The I_{max}, I_{min}, and J were averaged from all cross-section μCT images in the VOI using the CTan software. I_{max} and I_{min} represent the capacity of the bone to resist bending; J indicates the capacity of the bone to resist torsion.

Biomechanical whole-bone testing

Fractured and nonfractured femurs from SSRI-treated and control animals were subjected to biomechanical testing. Harvested femurs were wrapped in PBS-soaked gauze and stored at −20°C before biomechanical testing. Femurs were slowly returned back to room temperature in a water bath. Four-point bending analyses to failure were conducted using a materials testing machine (ElectroForce 3200; Bose, Eden Prairie, MN, USA) with a 245-N load cell and a linear variable displacement transducer (LVDT) with a range of ±6 mm. The upper span (loading) width was 3.0 mm and the lower span (support) width was 7.0 mm. Both the upper and lower contact anvils had a radius of 1.0 mm. Femurs were positioned posterior side down on the support anvils to cause bending in the sagittal plane. Four-point-bending was performed with a displacement control and linear loading ramp waveform at a 0.01 mm/s loading rate and data acquisition of 125 Hz.

Load-displacement curves were analyzed and maximum load (N), maximum displacement (mm), structural stiffness (N/mm), and toughness (N/mm^2) were assessed and normalized to body weight.

Histology and histomorphometry

Femurs and tibias were dissected and fixed overnight in 4% paraformaldehyde at 4°C. The samples were decalcified in 19% ethylenediaminetetraacetic acid (EDTA) for approximately 3 weeks at 4°C. Decalcified samples were dehydrated in a graded ethanol series, embedded into paraffin, and cut into 10-μm-thick sections. Pentachrome and aniline blue staining were used to detect osseous tissues as described.[11] Histochemistry for alkaline phosphatase (ALP) and tartrate-resistant acid phosphatase (TRAP) were performed with BM Purple substrate (Roche, Indianapolis, IN, USA) and Leukocyte Acid Phosphatase kit (Sigma, St. Louis, MO, USA), respectively, according to the manufacturers' instructions. Immunohistochemistry for Runx2 was performed using 25 μg/mL anti-Runx2 antibody (Rat

anti-human Runx2/Cbfa1 clone 232902; R&D Systems, Minneapolis, MN, USA) followed by 4 μg/mL donkey anti-rat biotin-conjugated secondary (Jackson ImmunoResearch, Westgrove, PA, USA), 1 μg/mL peroxidase-conjugated streptavidin (Jackson ImmunoResearch, Westgrove, PA, USA), and revealed by diaminobenzidine substrate (DAB-Plus Substrate; Thermo Fisher Scientific, Waltham, MA, USA). The sections were examined and photographed using a Leica digital imaging system.

In vivo calcein labeling and calculation of mineral apposition rate

For calcein labeling and mineral apposition rate (MAR) calculation, control ($n = 3$) and fluoxetine-treated ($n = 3$) mice were intraperitoneally injected with 30 mg/kg of Alizarin (Sigma-Aldrich) in a 2% sodium bicarbonate solution at POD 22 and with 20 mg/kg of calcein (Sigma-Aldrich) in a 2% sodium bicarbonate solution at POD 27 after femur fracture. On POD 28, the femurs were fixed in 4% paraformaldehyde for 48 hours, embedded in optimal cutting temperature compound (OCT) then cryosectioned at 100 μm thickness. The distance between the midpoints of the two labels was measured with ImageJ software (NIH, Bethesda, MD, USA; https://imagej.nih.gov/ij/), and values obtained were divided by the time between the Alizarin and calcein injections to obtain the MAR (μm/day).

SDS-PAGE and Western blotting

Bone fragments were collected from intact tibias, injured tibias from untreated mice, and injured tibias from fluoxetine-treated mice at POD 7. Tissue collection for the injured samples included a 3-mm segment, with the injury in the center; the intact specimens were collected from the same anatomic region of the tibia. After dissection, the harvested tissues were immediately frozen in liquid nitrogen then homogenized in radioimmunoprecipitation assay (RIPA) buffer (Thermo Fisher Scientific) and protease inhibitor cocktail (Sigma). Total protein was quantified with Bradford reagent using a bovine serum albumin (BSA) standard curve as reference. SDS–polyacrylamide gels at 8% to 16% concentration were loaded with 60 μg of lysate and proteins were blotted onto polyvinylidene fluoride (PVDF) membranes that were subsequently incubated for serotonin receptor 2B (2 μg/mL concentration, mouse anti-human 5-HT[2B]R clone A72-1; BD Pharmigen, San Jose, CA, USA), osteocalcin (1 μg/mL concentration, rabbit anti-human osteocalcin, sc-30044; Santa Cruz Biotechnology, Santa Cruz, CA, USA), Runx2 (1 μg/mL concentration, rabbit anti-mouse Runx2, sc-10758; Santa Cruz Biotechnology). GAPDH was probed as endogenous control (0.2 μg/mL concentration, mouse anti-GAPDH, 60004-1; Proteintech, Chicago, IL, USA). After primary antibody incubation overnight at 4°C, membranes were incubated with horseradish peroxidase (HRP)-conjugated secondary antibody (Bio-Rad, Hercules, CA, USA) and bands were detected with Clarity Western ECL Substrate (Bio-Rad) in an Odyssey Fc imaging system (LI-COR Biosciences, Lincoln, NE, USA) with 30 s exposure time. Protein expression was analyzed by measuring the intensity of detected bands compared to intact tibia samples and normalized to GAPDH with ImageJ software.

Bone marrow harvest for in vitro experiments

For the in vitro experiments, tibial and femoral bone marrow was extracted by centrifugation from untreated 12-week-old mice.[14] Cells were resuspended in growth media (GM), which consisted of DMEM (Thermo Fisher Scientific) containing 10% FBS (Thermo Fisher

Scientific) and 1% penicillin/streptomycin (Thermo Fisher Scientific), followed by plating in 75-mL tissue culture flasks. Media was replenished every 2 days. Approximately 1 week from harvest, the cells were trypsinized and passaged for the following assays.

Cellular proliferation assays

Cells were seeded in 96-well plates at a density of 2×10^4 cells per well in GM alone or containing 10 or 20 μM fluoxetine (Sigma). On day 3, BrdU assay (Abcam, Cambridge, UK) was performed according to the manufacturer's instruction. Wells were read on a Flex Station 3 microplate reader (Molecular Devices, Sunnyvale, CA, USA) at 450 nm. Data were collected with Soft Max Pro (Molecular Devices) software. Means and standard deviations (SDs) were calculated in GraphPad Prism 6 software (GraphPad Software, Inc., La Jolla, CA, USA).

Osteogenic differentiation

Cells were plated in 24-well plates with a density of 10,000 cells/well. After overnight attachment in GM, cells were treated with osteogenic differentiation media (OM) containing DMEM, 10% FBS, 100 μg/mL ascorbic acid, 10 mM β-glycerophosphate, and 1% penicillin/streptomycin. Cells were cultured in OM alone or containing 5, 10, or 20 μM fluoxetine. Media was replenished every 3 days. After 7 days, the cells were harvested and ALP activity was analyzed with an Alkaline Phosphatase Assay kit (Abcam, Cambridge, UK) following the manufacturer's instructions. After 14 days, Alizarin Red staining (ARS) was performed. ARS was quantified as described.[15] The samples were read on a Flex Station 3 microplate reader (Molecular Devices, Sunnyvale, CA, USA) at 405 nm in 96-well opaque-walled transparent-bottomed plates. Data were collected with Soft Max Pro (Molecular Devices) software. Means and SDs were calculated in GraphPad Prism 6 software.

RNA isolation and quantitative real-time PCR

Cells were plated in 24-well plates at a density of 10,000 cells/well. The cells were cultured in OM alone or containing 5, 10, or 20 μM fluoxetine. Media was replenished every 3 days. After 7 days, RNA was isolated (RNeasy Kit; Qiagen, Germantown, MD, USA), genomic DNA was removed (RNase-free DNase set; Qiagen) and the RNA reverse-transcribed (Omniscript RT Kit; Qiagen) with oligo-dT and random primers (Promega, Madison, WI, USA). Quantitative real-time PCR was carried out using the Applied Biosystems Step One Plus detection system (Thermo Fisher Scientific) and RT^2 SYBR Green ROX PCR Master Mix (Qiagen). Specific primers were designed based on PrimerBank (http://pga.mgh.harvard.edu/primerbank/) sequence (Table 1). Results are presented as $2^{-\Delta\Delta Ct}$ values normalized to the expression of 18S and negative control samples. All reactions were performed in triplicate; means and SDs were calculated in GraphPad Prism 6 software.

Serotonin assays

To test if the effects of fluoxetine on bone marrow OPCs are influenced by the presence of serotonin in the extracellular environment, mouse marrow cells were cultured in GM consisting of DMEM, 10% charcoal-stripped FBS (Corning, Manassas, VA, USA), and 1%

penicillin/streptomycin. Cells were treated with either 0.05% DMSO (vehicle), or 50 mM serotonin hydrochloride (Ser) (Abcam) alone, or with 5, 10, or 20 μM of fluoxetine alone or with both Ser and 5, 10, or 20 μM fluoxetine. BrdU assays were performed on day 3 as described. For osteogenic differentiation assays, cells were cultured in OM and treated as described above. After 7 days the cells were harvested and tested for ALP activity and gene expression of osteogenic markers by quantitative PCR as described. Alizarin red staining for mineralization was performed as described on day 14.

Statistical analysis

A priori power analysis to obtain statistical significance ($p = 0.05$, power 80%) resulted in an n of 4 for each group after body-size adjustment, expecting a 25% difference between the two groups.

Prism 7 (GraphPad Software, Inc., La Jolla, CA, USA) was used for statistical computations. A Student's t test was used for all comparisons in which there were two groups; ANOVA analyses followed by the Holms-Sidak correction for post hoc testing was applied for analyses in which there were two or more comparisons being made. Error bars represent SD. An asterisk symbol (*) denotes a p value <0.05.

Results

Effect of fluoxetine on murine femoral fracture healing

Histologic evaluation of femoral shaft fractures, stabilized with an intramedullary pin, at POD 14 revealed a large cartilaginous callus in both groups with woven bone formation at the peripheral edges of the callus (Fig. 1*A, B*). Histomorphometric analysis of the cartilage volume revealed no significant difference between the two groups (Fig. 1*E*). Histomorphometry of the bony callus using aniline blue to stain osteoid (Fig. 1*F*) revealed a similar callus volume in the control and the fluoxetine-treated femur fractures on POD 14.

On POD 28, the entire cartilaginous callus was replaced by bone in both experimental groups (Fig. 1*C, D*). However, a closer inspection of the microarchitecture of the bony regenerate revealed a striking difference. Although the bony callus of the control animals consisted of well-organized, thick trabeculae, the callus of the fluoxetine-treated mice showed fewer and thinner trabeculae (Fig. 1*C, D*; insets). We performed histomorphometry using aniline blue staining, which revealed that the bony callus volume was significantly smaller in the SSRI-treated animals (Fig. 1*F*, $p \leq 0.001$). Our histologic evaluation was complemented by μCT analysis of the femur fractures at POD 14 and 28. Three-dimensional reconstruction of the callus revealed woven bone formation in the periphery at POD 14 in both groups (Fig. 1*G, H*). Although the callus of the control animals had matured by POD 28 (Fig. 1*I*), the callus of the fluoxetine-treated fractures still exhibited a woven appearance (Fig. 1*J*). BV/TV was significantly reduced in the fluoxetine-treated femur fractures at POD 28 (Fig. 1*K*), and there was a trend toward a reduction in Tb.N, Tb.Th, and a trend toward an increase in Tb.Sp (Fig. 1*L–N*). Structural properties were calculated from the μCT data set, and revealed that the maximum and minimum bending moment of inertia (I_{max} and I_{min}, respectively) (Fig. 1*O*), as well as the polar moment of inertia (J) were significantly reduced

in the fluoxetine-treated animals, indicating a weaker, less mature bony regenerate. Finally, four-point bending testing was utilized to analyze structural properties of the fluoxetine and control-treated femurs on POD 28 (Fig. 1*P*). We observed a significant decrease in structural stiffness of the intact fluoxetine-treated femurs, whereas the fractured femurs displayed the same trend without reaching statistical significance ($p = 0.06$).

From this experiment we conclude that chronic SSRI use results in a smaller callus volume with thinner trabecular bone, while not affecting soft callus formation. The following experiments were aimed at identifying the mechanism by which fluoxetine treatment impaired fracture healing.

Fluoxetine treatment does not interfere with osteoclast activity during remodeling

First, we investigated whether fluoxetine treatment led to an increase in bone resorption during the remodeling phase, and in doing so resulted in a smaller fracture callus with thinner trabeculae. We performed TRAP staining to identify the number of activated osteoclasts. At both time points, there was no difference in the number and location of activated osteoclasts (Fig. 2*A*–*D*). Quantification of activated osteoclasts per millimeter woven bone surface revealed no significant difference between the control fractures and the fluoxetine-treated fractures (Fig. 2*E*). Therefore, increased bone resorption in response to chronic fluoxetine use can be ruled out as a cause for the observed phenotype.

Chronic SSRI treatment inhibits intramembranous bone formation

With a comparable sized cartilaginous foundation and similar osteoclast number, the difference in osseous callus volume may be attributed to reduced osteogenic differentiation and mineralization. To gain a better understanding of the effect of fluoxetine on osteogenic differentiation during fracture healing, we employed an in vivo model of intramembranous ossification. This monocortical tibial defect model heals reliably through primary bone formation, undergoing the typical stages of bone repair including inflammation, proliferation, angiogenesis, osteogenic differentiation, and remodeling. First, we assessed bone matrix deposition as a proxy for osteogenic differentiation. At both time points, the injury site was filled with woven bone (Fig. 3*A*–*D*). There was no cartilage formation present in any of the samples. Histomorphometric measurement of the osteoid revealed a significantly smaller bony regenerate after fluoxetine treatment at both consecutive time points (Fig. 3*E*). μCT analysis was used as a complementary analysis to evaluate bone matrix deposition at POD 7 and 14 (Fig. 3*F*–*I*), revealing a significantly smaller callus volume (BV/TV) at both time points (Fig. 3*J*). Trabecular number and trabecular thickness failed to demonstrate a statistically significant difference between the control and fluoxetine group (Fig. 3*K, L*).

Proliferation, osteogenic differentiation, and mineralization, but not remodeling, are decreased after SSRI treatment during intramembranous ossification

Using the previously described femoral shaft fracture model, we analyzed the MAR in transverse cross-sections of the mineralizing callus in calcein and Alizarin red–labeled fractured femurs at POD 28 (Fig. 4*A, B*). The MAR in fluoxetine-treated calluses was significantly lower compared to controls, which suggests that SSRI treatment reduced bone

matrix deposition by osteoblasts (Fig. 4*C*). In order to further understand the mechanism by which chronic fluoxetine treatment reduces intramembranous bone formation in vivo, we took a closer look at the different phases of intramembranous fracture repair in monocortical tibial defects. Previous studies have shown that the serotonin receptor 2B (5HTR2B) is present on osteoblasts.[16] It is still unknown, however, if 5HTR2B is upregulated in response to injury and if SSRI treatment affects receptor expression. Therefore, we first analyzed mRNA expression of 5HTR2B in uninjured tibias, injured tibias, and injured tibias in mice that were treated with fluoxetine. The expression of 5HTR2B was upregulated in tibial injuries at POD 7 compared to intact tibias, whereas the fluoxetine treatment resulted in downregulation of 5HTR2B to expression levels below that of uninjured controls (Fig. 4*D*). Second, we analyzed receptor presence on the protein level using Western blot analysis and confirmed the finding that the receptor was upregulated in response to injury, and fluoxetine resulted in a significant reduction of 5HTR2B (Fig. 4*E*). Next, we investigated whether fluoxetine treatment affected proliferation within the monocortical defects. Proliferating cell nuclear antigen (PCNA) staining revealed fewer PCNA-positive cells within the injury site, possibly indicating reduced proliferation of precursors cells within the defect at POD 7 (Fig. 4*F–H*). We then assessed the spatial *Runx2* expression by immunohistochemistry as a marker for early osteogenic differentiation. Numerous *runx2*-positive cells were observed within the injury site of control animals (Fig. 4*I*), whereas the fluoxetine-treated injury site exhibited fewer *runx2*-positive cells (Fig. 4*J*). We confirmed this finding by Western blot analysis, which revealed a statistically significant downregulation of *runx2* in the injury site by fluoxetine treatment (Fig. 4*K*). The late osteogenic differentiation marker osteocalcin was not altered, both on the transcriptional and protein level, in the injuries of both untreated and treated specimens compared to intact tibias (Fig. 4*K*, and data not shown). Finally, we assessed callus remodeling utilizing TRAP staining to visualize activated osteoclasts. At both day 7 and 14, there was no difference in average number of activated osteoclasts per millimeter bone surface, and therefore no difference in the resorptive aspect of remodeling, supporting our femur fracture data (Fig. 4*L–P*). From these analyses we conclude that chronic fluoxetine use negatively affects the proliferation, differentiation, and mineralization phase of intramembranous ossification during bone regeneration, without affecting the resorptive aspect of the remodeling phase.

In vitro effects of fluoxetine on bone marrow stromal cells

In order to identify the mechanism by which fluoxetine treatment impairs in vivo appendicular bone repair, we sought to further study its effect on bone marrow stromal cells (BMSCs) in vitro. We isolated cells from adult male 12-week-old C57B/L6 mice and subjected them to different doses of fluoxetine. We then assessed cell survival, proliferation, differentiation, and matrix deposition in vitro.

First, we assessed apoptosis using a TUNEL assay. Cells treated with 5 μM, 10 μM, and 20 μM fluoxetine did not show a significant change in frequency of cell death compared to the untreated cells (Fig. 5*A*). We then assessed cell proliferation using BrdU immunolabeling, and found no significant difference in cell division after fluoxetine treatment (Fig. 5*B*). Next, BMSCs were treated with osteogenic differentiation media and increasing doses of fluoxetine. After 14 days, Alizarin red staining and colorimetric analysis revealed a

statistically significant, dose-dependent decrease in matrix deposition, indicating decreased osteogenic differentiation in response to fluoxetine treatment (Fig. 5*C*). We confirmed this finding by performing an ALP assay (Fig. 5*D*) and gene expression analysis using qRT-PCR for *collagen type 1* (*col 1*), *osteocalcin* (*oc*), and *alkaline phosphatase* (*alp*) (Fig. 5*E*). Collectively, these data suggest a negative effect of fluoxetine on osteogenic differentiation in vitro.

Fluoxetine effect on BMSC differentiation is serotonin-independent

In order to further dissect the mechanism of action, we performed a series of in vitro experiments aimed at testing the direct effect of serotonin and SSRIs on bone cells. SSRIs block the cell membrane-bound serotonin reuptake channel, thus increasing the extracellular serotonin concentration. Osteoblast have been shown to express the serotonin receptors 5-HT1 and 5-HT2, members of a G protein-couple receptor family,[17] and therefore may be exposed to increased serotonin signaling in the presence of fluoxetine. In order to further dissect out the mechanism, we first sought to test the direct effect of serotonin alone on BMSCs. If SSRIs increase the extracellular serotonin concentration by blocking the transporter, then exogenous serotonin application should mimic this scenario of an increased extracellular serotonin concentration. BMSCs were grown in vitro in serotonin-free media and then exposed to 50 μM serotonin.[16] Proliferation was assessed using BrdU incorporation and revealed no significant difference between the control and the serotonin-treated cells (Fig. 6*A*). We then treated cells with varying doses of fluoxetine in the presence and absence of serotonin, and in both conditions proliferation was unchanged (Fig. 6*A*), suggesting that in vitro cell division is not affected by fluoxetine, by fluoxetine-mediated serotonin reuptake inhibition, or by direct serotonin treatment.

Next, we performed differentiation assays in the absence and presence of serotonin with varying doses of fluoxetine. After 7 days of culture in osteogenic differentiation media, we observed significantly lower ALP activity (Fig. 6*B*) and *collagen type I* expression (Fig. 6*C*) in fluoxetine-treated cultures both in the presence or absence of serotonin.

From these data we conclude that BMSC proliferation is not dependent or affected by serotonin or fluoxetine treatment. In contrast, after induction of osteogenic differentiation, fluoxetine treatment resulted in a serotonin-independent reduction in osteogenic differentiation, suggesting a direct, inhibitory effect of fluoxetine on osteoblasts.

Inhibitory effect of fluoxetine on osteoblasts persists after drug cessation

After demonstrating that fluoxetine inhibits osteoblast differentiation during fracture healing, and that this effect is serotonin-independent, we sought to investigate whether this negative effect can be halted by discontinuing the fluoxetine medication. This has important clinical implications, as one can envision discontinuing the medication in patients who sustain a fracture or require an orthopedic procedure in an attempt to restore osteogenic potential. We treated mice with fluoxetine for 3 weeks, and then stopped the medication and created femoral fractures (Fig. 7*A*). After 4 weeks, femurs underwent μCT analysis (Fig. 7*B–D*). Similar to femur fractures in mice that received continued fluoxetine, femur fractures in mice with interrupted fluoxetine treatment showed a reduced callus volume and

trabecular number, whereas trabecular thickness and spacing was unchanged in comparison to the untreated controls (Fig. 7*E–H*). A closer look at the 3D reconstructions of the femur fractures in mice with discontinued fluoxetine treatment revealed a persistent fracture gap, spanning the entire callus (Fig. 7*D*). We further analyzed the bones by histology, and observed a persistent cartilaginous core surrounding the non-union site (Fig. 7*I–K*). Although none of the specimens in the control or fluoxetine-treated group had any evidence of cartilage at 28 days postfracture, the fluoxetine discontinued group consistently showed cartilaginous callus in the center portion of the callus (Fig. 7*L*). Aniline blue staining confirmed the lack of union in the discontinued group, and histomorphometric bone analysis revealed a slight increase of bone volume in the discontinued group compared to the treated group; however, callus size did not reach that of the control callus (Fig. 7*M–P*). Again, we investigated whether osteoclastic activity was responsible for the finding of reduced callus size, maintained cartilage tissue, and persistent fracture gap. Despite an abundance of osteoclasts at the fracture edges, there was no significant difference in the number of osteoclasts per millimeter callus between the three groups (Fig. 7*Q–T*). Finally, we assessed ALP activity as a proxy for osteoblastic differentiation. Although the control and continuously treated group presented labeling for ALP activity throughout the remodeling callus, the “fluoxetine discontinued” group exhibited intense ALP labeling at the fracture edges (Fig. 7*U–W*). Together these data suggest that discontinuing fluoxetine treatment prior to a fracture does not recover the endogenous regenerative potential of the osteoprogenitor cells. In fact, it may even lead to an overall delay of the program of endochondral ossification with maintained soft callus and lack of fracture union.

Discussion

Animal research and human clinical data have clearly shown that chronic SSRI use leads to osteoporosis, thus putting patients at risk for a fragility fracture.[6,18–20] Our data provide strong evidence that besides affecting bone homeostasis, SSRIs negatively affect bone regeneration. Here, we demonstrate that both endochondral and intramembranous ossification are delayed in response to fluoxetine treatment, which may have profound clinical implications. Our analysis revealed that chronic fluoxetine use decreased proliferation and osteogenic differentiation in two disparate models of fracture repair, while not affecting chondrogenic differentiation and remodeling. Analysis of the fracture callus of SSRI-treated animals revealed an overall reduced cross-sectional moment of inertia and structural stiffness, suggesting a callus of reduced biomechanical strength.

This study is the first to examine the in vivo effects of SSRIs on the complex program of appendicular bone healing. Previous in vitro studies have analyzed the effect of SSRI on osteoblasts,[21,22] osteocytes,[23] osteoclasts,[21] and various bone cell lines,[24] and most of these studies confirmed our findings of reduced osteogenic differentiation with decreased mineral deposition. Our in vitro study provides evidence that the SSRI effect on bone cells is direct in nature rather than serotonin-dependent, and this is similar to the findings presented by Hodge and colleagues.[21] Here, the authors tested fluoxetine, sertraline, paroxetine, fluvoxamine, and citalopram on osteoclasts and osteoblasts, and were able to demonstrate that each SSRI differentially inhibited osteoclast and osteoblast maturation and mineralization. Citalopram, however, did not negatively affect ALP activity and

mineralization, potentially offering an alternative antidepressant for patients with challenging fractures, non-unions, and patients at risk. Our in vivo data show that osteoclast density was not affected by fluoxetine treatment, indicating that the osteoblast/osteoclast axis is not affected by fluoxetine treatment.

A study by Mortazavi and colleagues[25] investigated the effect of two different doses of fluoxetine on bone regeneration in a parietal critical-size defect model in rats. Treatment was started immediately after injury and persisted for a total of 8 weeks. The authors report an increase in bone formation after fluoxetine treatment, which is in stark contrast to our findings and the results of the abovementioned references. A possible explanation for this difference in outcome may be the variance in the fluoxetine treatment protocol. Although Mortazavi and colleagues[25] administered fluoxetine immediately postinjury, the current study utilized a model of chronic fluoxetine use. In addition, cells from the cranium and the appendicular skeleton differ not only in their embryonic origin, but also respond differently to drugs/growth factors,[26,27] which may have resulted in these contrasting findings.

Most interesting in our current study, the negative effect of fluoxetine treatment on bone cells seemed to persist for a prolonged time after discontinuation of the drug. Bolo and colleagues[28] showed that fluorinated SSRIs, such as fluvoxamine and fluoxetine, sequester into the bone/bone marrow compartment, where they were detectable months after discontinuation of the therapy. In addition, the concentration within the bone marrow compartment was measured to be an order of magnitude higher than in plasma. Although there was a rapid clearance of the drug from the plasma compartment after cessation, the bone/bone marrow concentrations remained high.[28] And, for still unknown reasons, discontinuing the SSRI in this current mouse model resulted in a complete failure of successful bone healing and establishment of non-unions with persistent soft callus. If, in fact, this observation translates into clinical practice, then one needs to consider continuation of the drug despite its obvious negative effect on bone healing, as the consequence of discontinuation is more debilitating. Future research will further analyze this amplified, negative effect of fluoxetine on bone healing after drug cessation.

Delayed unions and non-unions are associated with a significant mental burden, known to trigger depression. In light of these findings, surgeons taking care of patients on SSRIs, who undergo treatment for delayed unions or non-unions may consider converting them to an antidepressant of another class in order to avoid the negative effects outlined in this study. However, one has to consider the prolonged clearance period from the bone/bone marrow compartment of the fluorinated SSRI.

In summary, data from this study and others provide strong evidence that chronic SSRI use leads to osteoporosis, which is associated with an increased fracture risk. Our current study shows that SSRIs negatively affect bone healing by inhibiting proliferation, osteoblast differentiation, and mineralization. Therefore, special emphasis should be paid to this patient population in an attempt to initially prevent bone loss, and then, if required, to optimize fracture healing.

Supplementary Material

Refer to Web version on PubMed Central for supplementary material.

Acknowledgments

We thank Ripa Chowdhury (New York University College of Dentistry) for assistance with the μCT imaging (supported by NIH 1 S10 OD010751-01A1), Jessica Lavery for the assistance with the statistical analysis, and Matin Lendhey for the biomechanical testing.

Disclosures

PL is a consultant for Ankasa Regenerative Therapeutics, Inc. PL also receives research support from the National Institutes of Health (NIH), the Musculoskeletal Transplant Foundation (MTF), and the Orthopaedic Trauma Association (OTA).

References

1. Feuer AJ, Demmer RT, Thai A, Vogiatzi MG. Use of selective serotonin reuptake inhibitors and bone mass in adolescents: an NHANES study. Bone. 2015; 78:28–33. [PubMed: 25940460]
2. Wysowski DK, Governale LA, Swann J. Trends in outpatient prescription drug use and related costs in the US: 1998–2003. Pharmacoeconomics. 2006; 24(3):233–236. [PubMed: 16519545]
3. Rizzoli R, Cooper C, Reginster J-Y, et al. Antidepressant medications and osteoporosis. Bone. 2012; 51(3):606–613. [PubMed: 22659406]
4. Richter T, Paluch Z, Alusik S. The non-antidepressant effects of citalopram: a clinician's perspective. Neuro Endocrinol Lett. 2014; 35(1):7–12. [PubMed: 24625921]
5. Lanteigne A, Sheu Y-H, Stürmer T, et al. Serotonin-norepinephrine reuptake inhibitor and selective serotonin reuptake inhibitor use and risk of fractures: a new-user cohort study among US adults aged 50 years and older. CNS Drugs. 2015; 29(3):245–252. [PubMed: 25708711]
6. Warden SJ, Robling AG, Sanders MS, Bliziotes MM, Turner CH. Inhibition of the serotonin (5-hydroxytryptamine) transporter reduces bone accrual during growth. Endocrinology. 2005; 146(2): 685–693. [PubMed: 15539550]
7. Banovic M, Bordukalo-Niksic T, Balija M, Cicin-Sain L, Jernej B. Platelet serotonin transporter (5HTt): physiological influences on kinetic characteristics in a large human population. Platelets. 2010; 21(6):429–438. [PubMed: 20528260]
8. Rauma PH, Honkanen RJ, Williams LJ, Tuppurainen MT, Kroger HP, Koivumaa-Honkanen H. Effects of antidepressants on postmenopausal bone loss - a 5-year longitudinal study from the OSTPRE cohort. Bone. 2016; 89:25–31. [PubMed: 27179631]
9. Dulawa SC, Holick KA, Gundersen B, Hen R. Effects of chronic fluoxetine in animal models of anxiety and depression. Neuropsychopharmacology. 2004; 29(7):1321–1330. [PubMed: 15085085]
10. Bonnarens F, Einhorn TA. Production of a standard closed fracture in laboratory animal bone. J Orthop Res. 1984; 2(1):97–101. [PubMed: 6491805]
11. Leucht P, Kim J-B, Wazen R, et al. Effect of mechanical stimuli on skeletal regeneration around implants. Bone. 2007; 40(4):919–930. [PubMed: 17175211]
12. Minear S, Leucht P, Jiang J, et al. Wnt proteins promote bone regeneration. Sci Transl Med. 2010; 2(29):29ra30.
13. O'Neill KR, Stutz CM, Mignemi NA, et al. Micro-computed tomography assessment of the progression of fracture healing in mice. Bone. 2012; 50(6):1357–1367. [PubMed: 22453081]
14. Kelly NH, Schimenti JC, Patrick Ross F, van der Meulen MC. A method for isolating high quality RNA from mouse cortical and cancellous bone. Bone. 2014; 68:1–5. [PubMed: 25073031]
15. Hill CR, Yuasa M, Schoenecker J, Goudy SL. Jagged1 is essential for osteoblast development during maxillary ossification. Bone. 2014; 62:10–21. [PubMed: 24491691]
16. Collet C, Schiltz C, Geoffroy V, Maroteaux L, Launay JM, de Vernejoul MC. The serotonin 5-HT2B receptor controls bone mass via osteoblast recruitment and proliferation. FASEB J. 2008; 22(2):418–427. [PubMed: 17846081]

17. Michalowska M, Znorko B, Kaminski T, Oksztulska-Kolanek E, Pawlak D. New insights into tryptophan and its metabolites in the regulation of bone metabolism. J Physiol Pharmacol. 2015; 66(6):779–791. [PubMed: 26769827]
18. Warden SJ, Hassett SM, Bond JL, et al. Psychotropic drugs have contrasting skeletal effects that are independent of their effects on physical activity levels. Bone. 2010; 46(4):985–992. [PubMed: 20060080]
19. Warden SJ, Nelson IR, Fuchs RK, Bliziotes MM, Turner CH. Serotonin (5-hydroxytryptamine) transporter inhibition causes bone loss in adult mice independently of estrogen deficiency. Menopause. 2008; 15(6):1176–1183. [PubMed: 18725867]
20. Fernandes BS, Hodge JM, Pasco JA, Berk M, Williams LJ. Effects of depression and serotonergic antidepressants on bone: mechanisms and implications for the treatment of depression. Drugs Aging. 2016; 33(1):21–25. [PubMed: 26547857]
21. Hodge JM, Wang Y, Berk M, et al. Selective serotonin reuptake inhibitors inhibit human osteoclast and osteoblast formation and function. Biol Psychiatry. 2013; 74(1):32–39. [PubMed: 23260229]
22. Cray JJ Jr, Weinberg SM, Parsons TE, Howie RN, Elsalanty M, Yu JC. Selective serotonin reuptake inhibitor exposure alters osteoblast gene expression and craniofacial development in mice. Birth Defects Res A Clin Mol Teratol. 2014; 100(12):912–923. [PubMed: 25308507]
23. Bliziotes MM, Eshleman AJ, Zhang XW, Wiren KM. Neurotransmitter action in osteoblasts: expression of a functional system for serotonin receptor activation and reuptake. Bone. 2001; 29(5):477–486. [PubMed: 11704501]
24. Salai M, Somjen D, Gigi R, Yakobson O, Katzburg S, Dolkart O. Effects of commonly used medications on bone tissue mineralisation in SaOS-2 human bone cell line: an in vitro study. Bone Joint J. 2013; 95-B(11):1575–1580. [PubMed: 24151282]
25. Mortazavi SH, Khojasteh A, Vaziri H, Khoshzaban A, Roudsari MV, Razavi SH. The effect of fluoxetine on bone regeneration in rat calvarial bone defects. Oral Surg Oral Med Oral Pathol Oral Radiol Endod. 2009; 108(1):22–27. [PubMed: 19272809]
26. Quarto N, Wan DC, Kwan MD, Panetta NJ, Li S, Longaker MT. Origin matters: differences in embryonic tissue origin and Wnt signaling determine the osteogenic potential and healing capacity of frontal and parietal calvarial bones. J Bone Miner Res. 2010; 25(7):1680–1694. [PubMed: 19929441]
27. Leucht P, Kim JB, Amasha R, James AW, Girod S, Helms JA. Embryonic origin and Hox status determine progenitor cell fate during adult bone regeneration. Development. 2008; 135(17):2845–2854. [PubMed: 18653558]
28. Bolo NR, Hode Y, Macher JP. Long-term sequestration of fluorinated compounds in tissues after fluvoxamine or fluoxetine treatment: a fluorine magnetic resonance spectroscopy study in vivo. MAGMA. 2004; 16(6):268–276. [PubMed: 15042463]

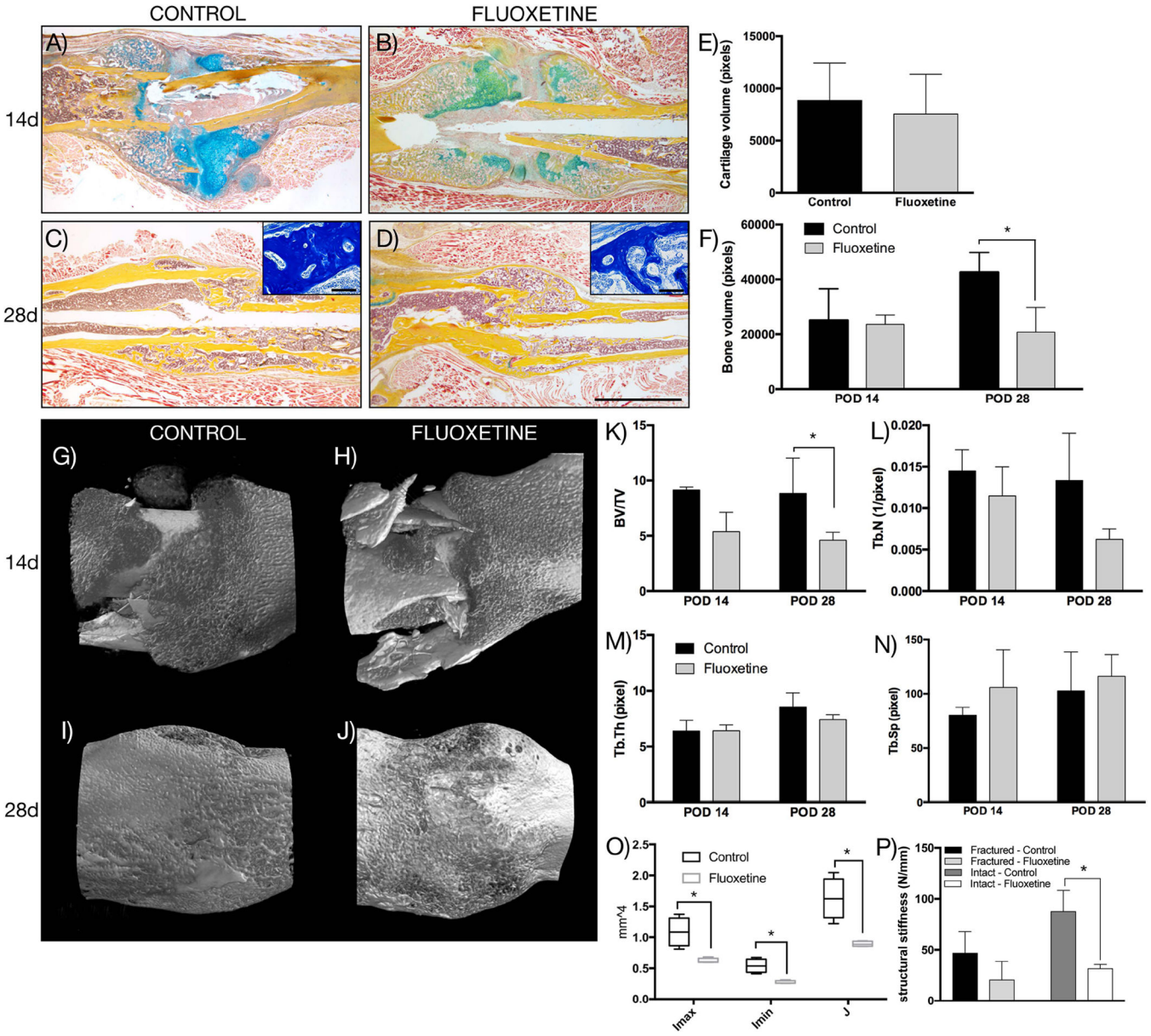

Fig. 1.

Fluoxetine inhibits osteogenic phase of endochondral ossification. (*A–D*) Pentachrome staining of representative longitudinal sections through fracture callus. Insets in *C* and *D* show high magnification of aniline blue staining of the callus region demonstrating difference in trabecular architecture. (*E*) Histomorphometry of cartilage volume at day 14 and (*F*) bony callus at day 14 and 28 ($n = 4$, $p < 0.05$). (*G–J*) 3D reconstruction of μCT analysis of the fracture callus at 14 and 28 days ($n = 4$). (*K–N*) Analysis of μCT data showing BV/TV, Tb.N, Tb.Th, and Tb.Sp. (*O*) Maximum and minimum bending moment of inertia (I_{max} and I_{min}, respectively), as well as the polar moment of inertia, *J*, of at POD 28 ($n = 4$, $p < 0.01$). (*P*) Four-point bending analysis of uninjured and injured femurs (POD 28) ($n = 4$). Asterisk denotes statistical significance. Scale bar = 2 mm, 100 μm in insets. d =

day; POD = postoperative day; BV/TV = bone volume/total volume; Tb.N = trabecular number; Tb.Th = trabecular thickness; Tb.Sp = trabecular spacing.

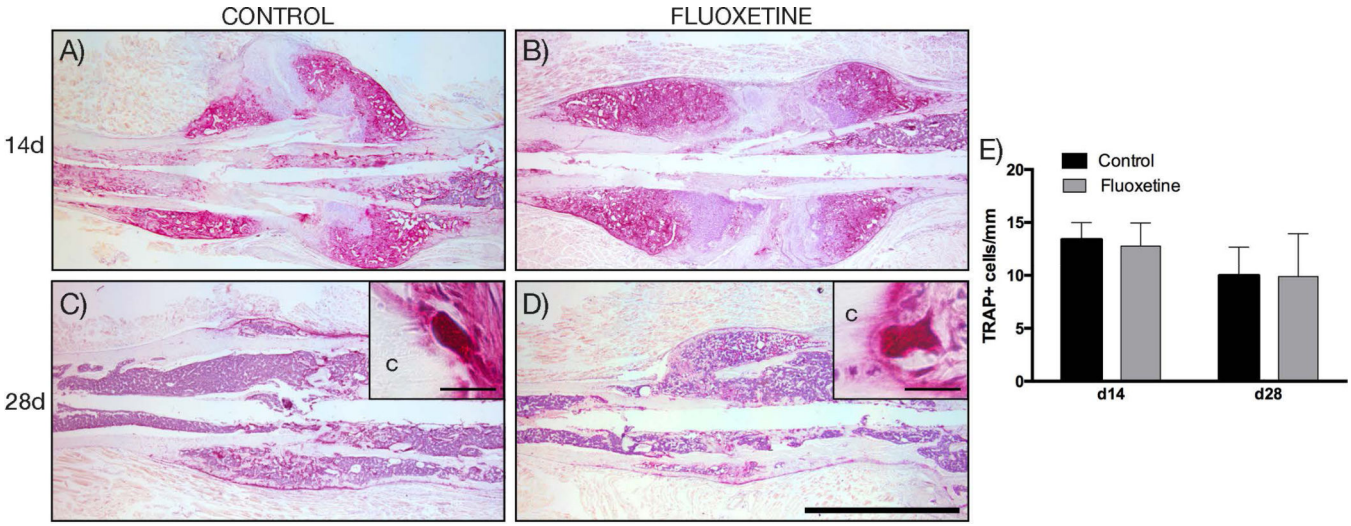

Fig. 2.

Decreased callus volume of femur fractures in fluoxetine treated mice is not a result of increased osteoclast number. (*A*–*D*) TRAP staining of the fracture callus at 14 and 28 days after fracture. (*E*) Histomorphometric quantification of activated, bone lining osteoclasts ($n = 4$). Scale bar = 2 mm. c = cortical bone; TRAP = tartrate-resistant acid phosphatase.

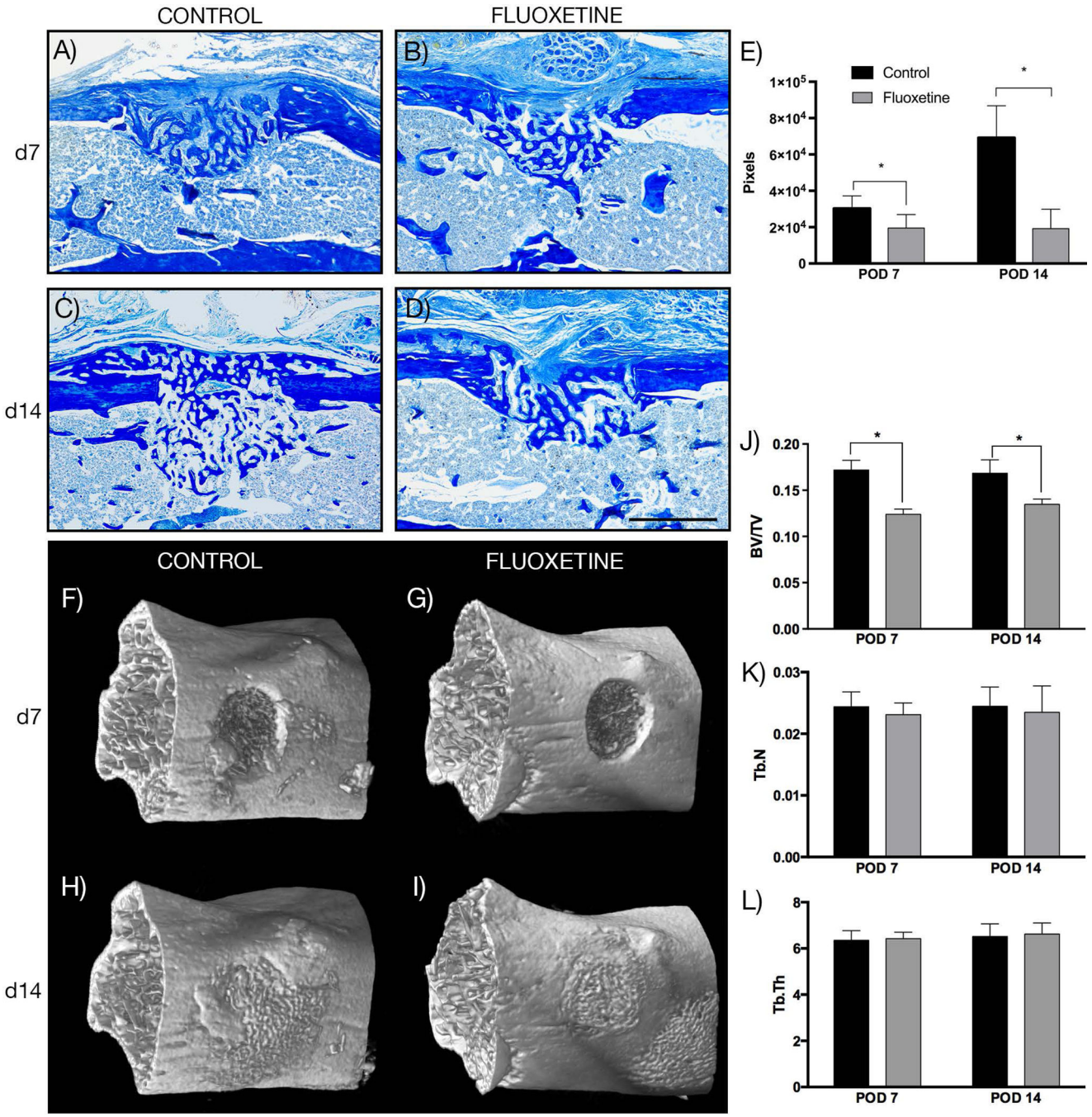

Fig. 3.

Fluoxetine treatment disrupts intramembranous bone formation and results in smaller bony regenerate. (*A*–*D*) Aniline blue staining of representative longitudinal sections through monocortical defect sites. (*E*) Histomorphometric analysis of bony regenerate size ($n = 4$, $p = 0.04$ [POD7], $p < 0.001$ [POD14]). (*F*–*I*) 3D reconstruction of μCT analysis of the monocortical defect site at 7 and 14 days. (*J*–*L*) Analysis of μCT data showing BV/TV, Tb.N, Tb.Th, and Tb.Sp ($n = 4$, $p < 0.05$). Asterisk denotes statistical significance. Scale bar

= 500 μm. d = day; POD = postoperative day; BV/TV = bone volume/total volume; Tb.N = trabecular number; Tb.Th = trabecular thickness; Tb.Sp = trabecular spacing.

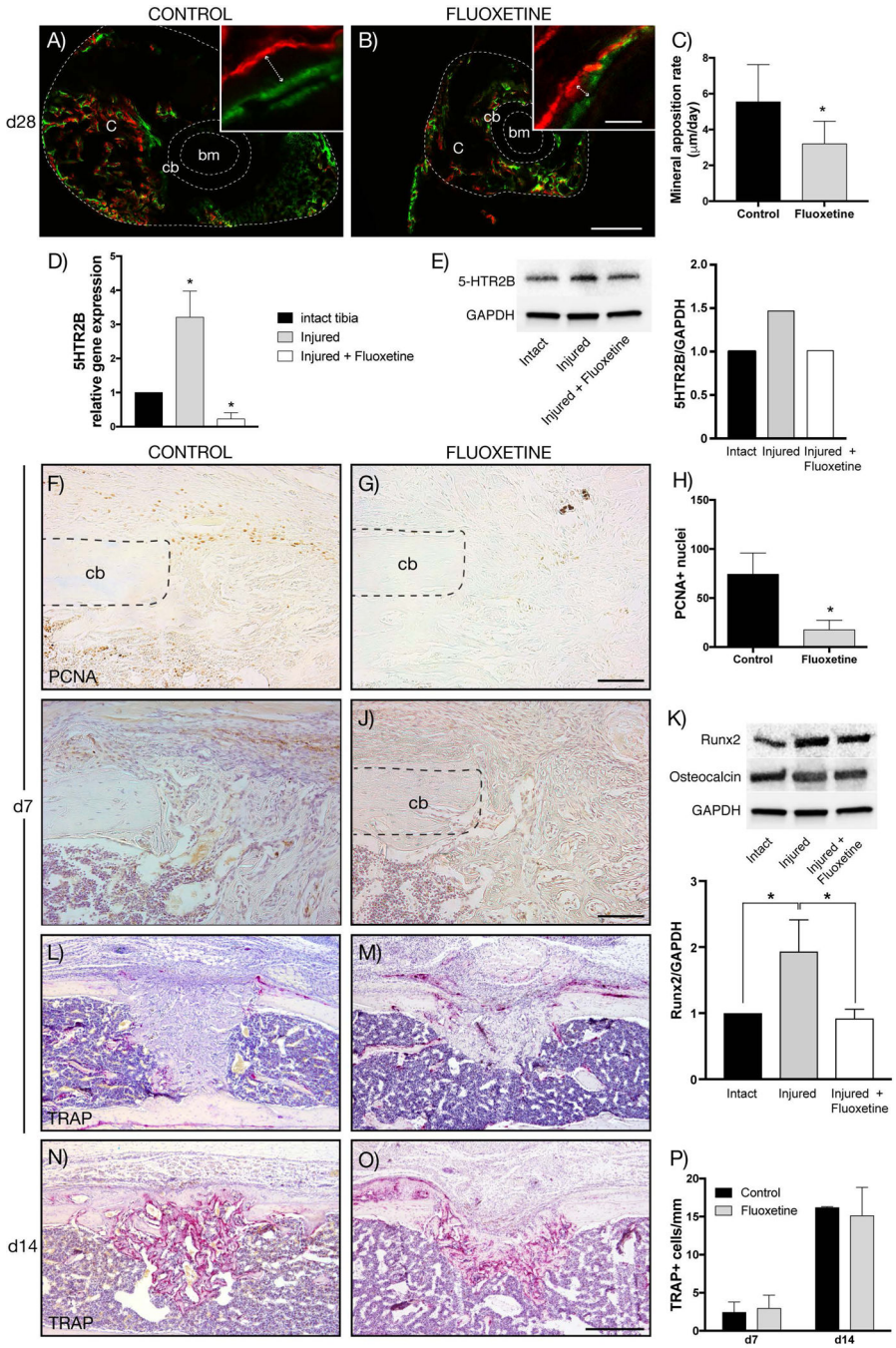

Fig. 4.

Proliferation, osteogenic differentiation, and mineralization is decreased in fluoxetine treated mice, while osteoclast activity remains unchanged. (*A, B*) Alizarin red (red) and calcein (green) labeling of fracture callus (outer dotted line) at POD 28. Inserts show representative high-magnification images used for quantification (arrow depicts ossification front). (*C*) Dynamic histomorphometry quantifying the mineral apposition rate of control and fluoxetine treated mice ($n = 3$, $p < 0.05$). (*D, E*) mRNA and protein expression of 5HTR2B is upregulated in response to injury at d7, while fluoxetine treatment resulted in

downregulation ($n = 3$). (*F, G*) Immunohistochemistry for PCNA revealing decreased proliferation in fluoxetine-treated animals. (*H*) Quantification of PCNA-positive cells within the injury site ($n = 4$, $p < 0.001$). (*I, J*) *Runx2* immunolabeling at POD 7 revealed an abundance of runx2-positive cells within the periosteum and the injury site of control animals, whereas the fluoxetine-treated animals exhibited fewer runx2-positive cells. (*K*) This finding was confirmed by Western blot analysis, which showed a significant decrease in Runx2 protein levels within the injury site of fluoxetine-treated animals compared to control animals. Osteocalcin levels were unchanged among groups. (*L–O*) Representative longitudinal section stained for TRAP in fluoxetine-treated and control animals at 7 and 14 days postsurgery. Quantification of activated osteoclasts reveals no significant differences between the two groups. Asterisk denotes statistical significance ($p \leq 0.05$). Scale bar = 300 μm (*A, B*), 20 μm (*A, B*, insets), 100 μm (*F, G, I, J*), 500 μm (*L–O*). bm = bone marrow; c = callus; cb = cortical bone; d = day; oc = osteocalcin; PCNA = proliferating cell nuclear antigen; POD = postoperative day; 5HTR2B = serotonin receptor 2B.

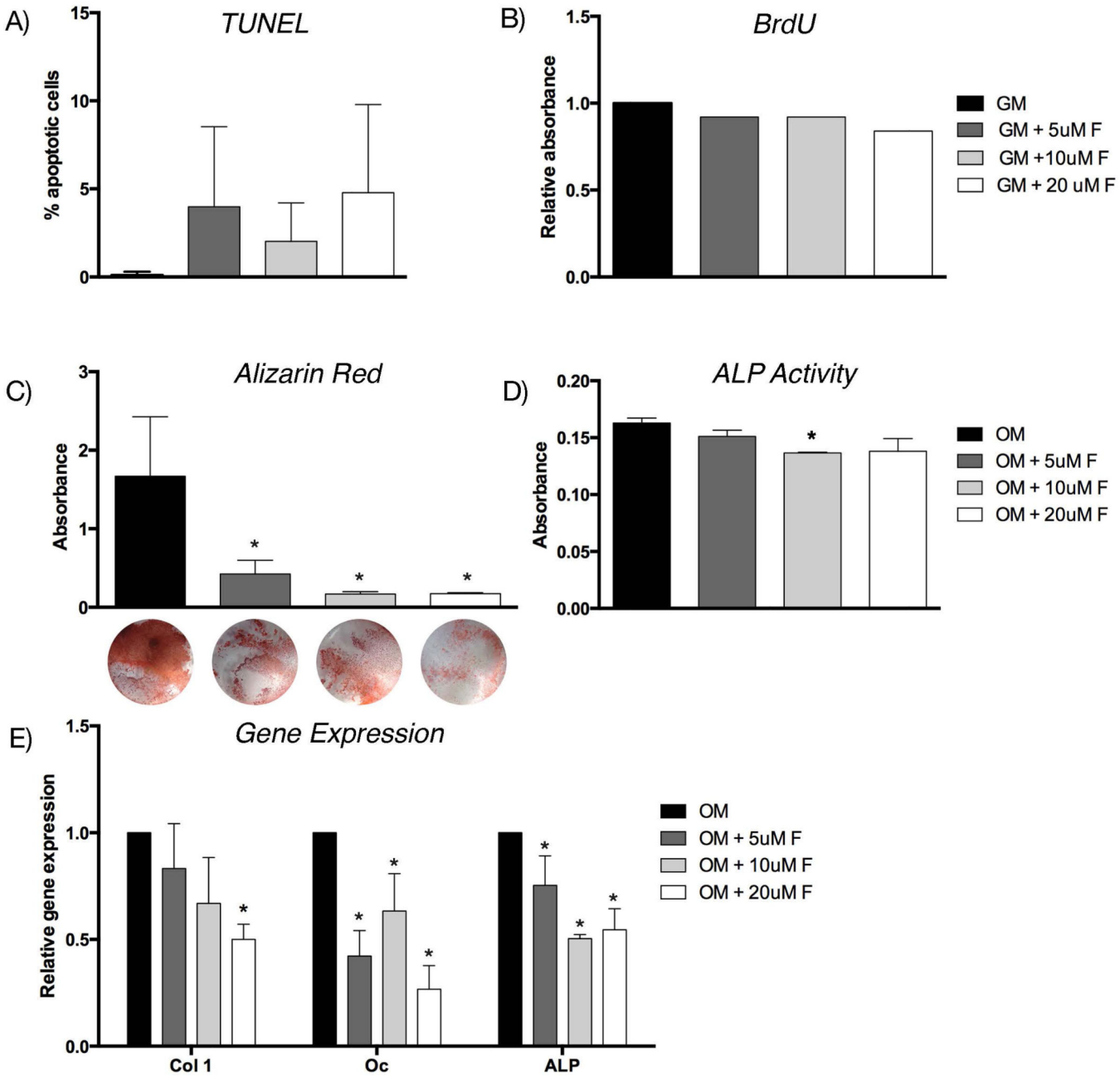

Fig. 5.

Fluoxetine inhibits osteogenic differentiation of bone marrow stromal cell in vitro. (*A*) TUNEL assay of BMSCs in GM with varying concentrations of fluoxetine. (*B*) Proliferation assay using BrdU labeling of BMSC in growth media with varying concentrations of fluoxetine. (*C*) Alizarin red staining was quantified using absorbance, representative images of the mineralization assay are shown below. (*D*) ALP activity of BMSCs in OM and varying concentrations of fluoxetine. (*E*) Gene expression of *col 1, oc*, and *ALP* in BMSC cultured in OM and fluoxetine. Asterisk denotes statistical significance ($p < 0.05$), statistical comparison against growth/osteogenic media control. alp = alkaline phosphatase; BrdU =

Bromodeoxyuridine; col 1 = collagen type 1; f = fluoxetine; GM = growth media; oc = osteocalcin; OM = osteogenic differentiation media; BMSC = bone marrow stromal cell.

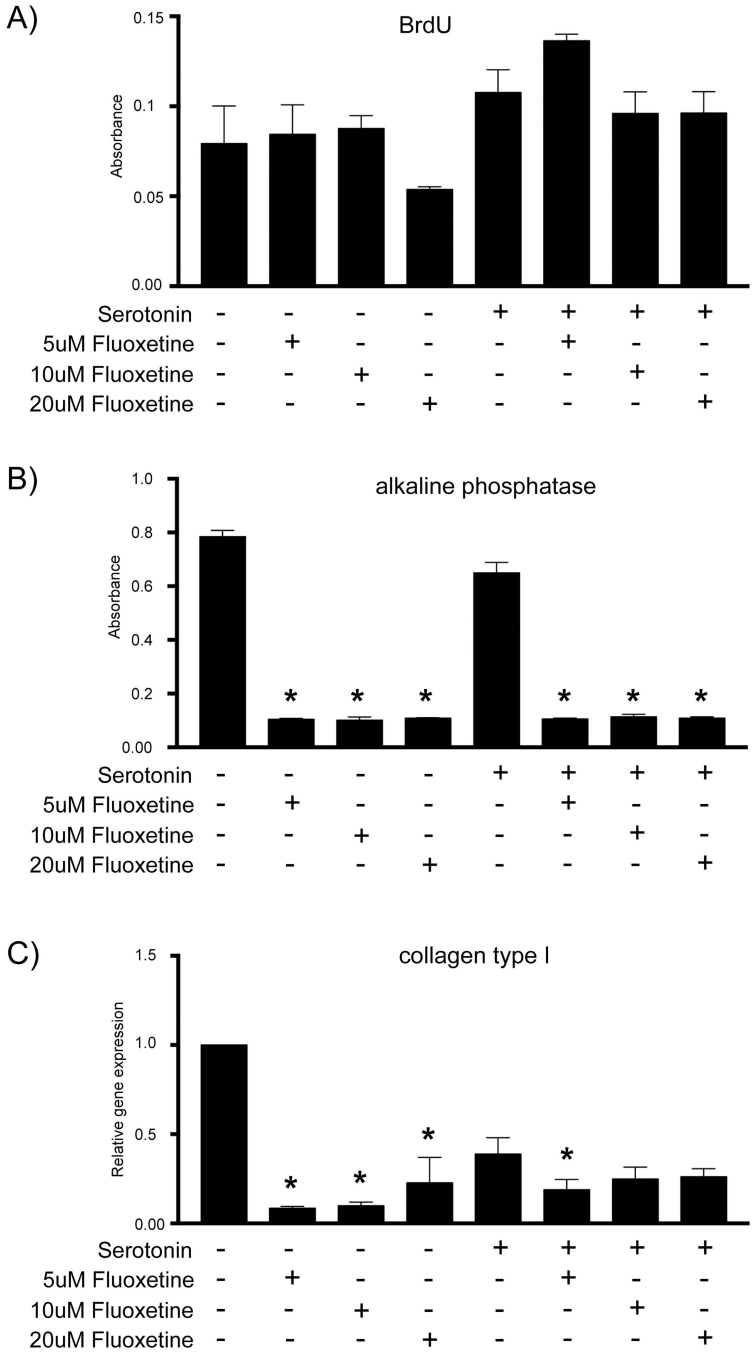

Fig. 6.

Inhibitory effect of fluoxetine on osteogenic differentiation in vitro is serotonin-independent. (*A*) Proliferation assay, (*B*) alkaline phosphatase assay, and (*C*) gene expression of *collagen type 1* of BMSCs in serotonin-free media with supplementation of serotonin and varying doses of fluoxetine as outlined in the tables below the figures. Asterisk denotes statistical significance ($p < 0.05$), statistical comparison against media control. F = fluoxetine; ser = serotonin; BMSC = bone marrow stromal cell.

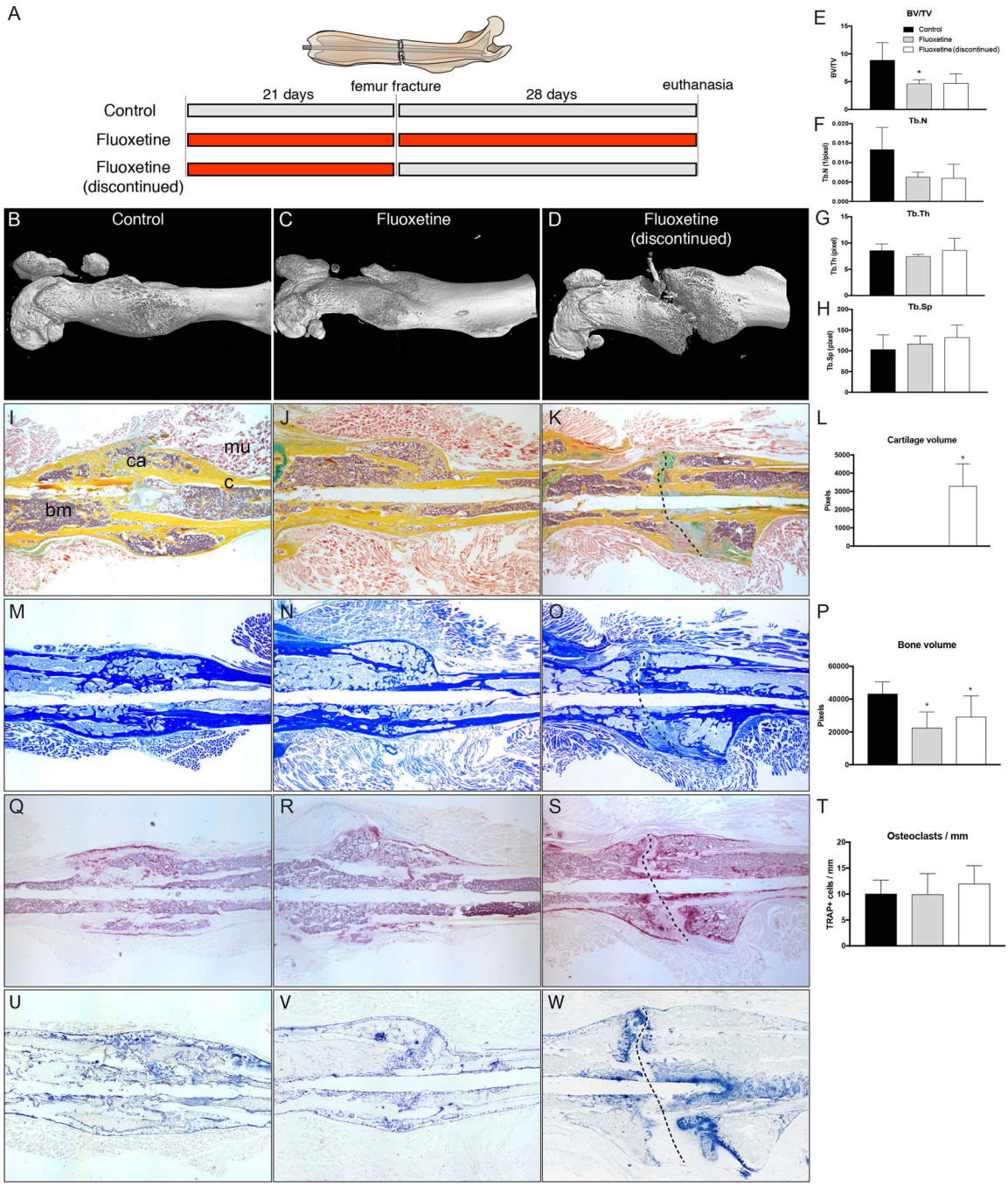

Fig. 7.

Discontinuation of fluoxetine treatment results in bony non-union in femoral fracture model. (*A*) Schematic representing the three experimental groups. (*B–H*) μCT analyses of femur fractures in control, fluoxetine treated, and fluoxetine-discontinued animals showing prolonged effect of SSRI on bone healing and incomplete fracture healing with callus gap ($n = 4$, $p < 0.05$). (*I–K*) Pentachrome staining of representative section showing fibrous non-union formation (dotted line in *K, O, S, W*) in the drug cessation group. (*L*) Histomorphometric evaluation of the callus reveals persistent cartilage at POD 28 in the

fluoxetine-discontinued group ($n = 4$, $p < 0.05$). (*M–P*) Aniline blue staining demonstrating bony regenerate size in the three experimental groups. Histomorphometry shows mild increase in bone formation, but still significantly below the control ($n = 4$, $p < 0.05$). (*Q–T*) TRAP staining and analysis confirmed that the phenotype is not caused by an increase in osteoclastic resorption ($n = 4$, $p < 0.04$). (*U, V*) Alkaline phosphatase staining indicating ongoing osteogenic differentiation, with increased staining at the ossification front within the persistent fracture gap (*W*, dotted line). Scale bar = 2 mm. Asterisk denotes statistical significance ($p < 0.05$). bm = bone marrow; BV/TV = bone volume/total volume; c = cortical bone; ca = callus; d = day; mu = muscle; POD = postoperative day; Tb.N = trabecular number; Tb.Sp = trabecular spacing; Tb.Th = trabecular thickness.

Table 1

PCR Primers

Primer name	Sequence (5′–3′)
18S FOR	ACGAGACTCTGGCATGCTAACTAGT
18S REV	CGCCACTTGTCCCTCTAAGAA
Alkaline phosphatase FOR	ACCTTGACTGTGGTTACTGC
Alkaline phosphatase REV	CATATAGGATGGCCGTGAAGG
Osteocalcin FOR	TGTGACGAGCTATCAAACCAG
Osteocalcin REV	GAGGATCAAGTTCTGGAGAGC
Collagen I FOR	CAGTCGATTCACCTACAGCACG
Collagen I REV	GGGATGGAGGGAGTTTACACG
5-HTR2B FOR	CTGGAACGGCCAAATGTACT
5-HTR2B REV	CCTCCGTTTGTCCTTGGTAA

All primers were purchased from Integrated DNA Technologies.

FOR = forward; REV = reverse.